Wen-Jun Hu, Mei-Fu Zhou, John Malpas, and Zhong-Yuan Ren, 2021, High-Ca boninitic melt inclusions in lavas of the Troodos ophiolite and a reappraisal of genetic relationships between different lava types: GSA Bulletin, https://doi.org/10.1130/B35717.1

Supplemental Material

Table A1. Microprobe analyses of olivine phenocrysts in the Margi picritic lavas of the Troodos ophiolite, Cyprus

Table A2. Microprobe analyses of spinels and host olivines in the Margi picritic lavas of the Troodos ophiolite, Cyprus

Table A3. Chemical compositions of olivine-hosted melt inclusions in the Margi picritic lavas of the Troodos ophiolite, Cyprus

Table A4. Pb isotopic ratios of measured and age-corrected of olivine-hosted melt inclusions in the Margi picritic lavas of the Troodos ophiolite, Cyprus

Table A5. Calculated compositions, temperature and pressure of primary magma of boninite and the LPL in the Troodos ophiolite. Data of the melt inclusion of the LPL are from Portnyagin et al. (1997). Temperature and pressure are calculated by the method of Katz et al. (2003), Lee et al (2009), and Herzberg and Asimow (2015).

Table A6. Literature data of melt inclusions of the Troodos ophiolite, Cyprus. Data are from Sobolev et al. (1991) and Portnyagin et al. (1996, 1997).

Table A7. Literature data of volcanic glass of the Troodos ophiolite, Cyprus. Data are from Portnyagin et al. (1997), Pearce and Robinson (2010), Osozawa et al. (2012), Regelous et al. (2014), Woelki et al. (2018, 2019 and 2020), and Golowin et al. (2017).

Figure A1. Comparison of the Fo of olivine in equilibrium with the melt inclusion against the Fo of the olivine host. Fo of the equilibrium olivine were calculated by measured data of melt inclusions with assuming KD=[(XFe$_{ol}$/XMg$_{liq}$)/ (XMg$_{ol}$/XFe$_{liq}$)]=0.3.

Figure A2. Comparison of the melt inclusion against the boninitic glass in the Troodos ophiolite. Data of the boninitic glass in the Troodos ophiolite are from Pearce and Robinson (2010), Osozawa et al. (2012), and Woelki et al. (2018, 2019 and 2020).

Figure A3. Major composition of volcanic glass in the Troodos ophiolite. Data are from Portnyagin et al. (1997), Pearce and Robinson (2010), Osozawa et al. (2012), Regelous et al. (2014), Golowin et al. (2017), and Woelki et al. (2018, 2019 and 2020).

Figure A4. Primitive mantle normalized trace element patterns of the boninitic glass in the Troodos ophiolite. The normalization values are from Sun and McDonough (1989).

REFERNCES CITED

Herzberg, C., and Asimow, P.D., 2015, PRIMELT 3 MEGA. XLSM software for primary magma calculation: peridotite primary magma MgO contents from the liquidus to the solidus: Geochemistry Geophysics Geosystems, v. 16, p. 563–578, https://doi.org/10.1002/2014GC005631.

Golowin, R., Portnyagin, M., Hoernle, K., Sobolev, A., Kuzmin, D., and Werner, R., 2017, The role and conditions of second-stage mantle melting in the generation of low-Ti tholeiites and boninites: The case of the Manihiki Plateau and the Troodos ophiolite: Contributions to Mineralogy and Petrology, v. 172, no. 104, https://doi.org/10.1007/s00410-017-1424-3.

Katz, R.F., Spiegelman, M., and Langmuir, C.H., 2003, A new parameterization of hydrous mantle melting: Geochemistry Geophysics Geosystems, v. 4, 1073, https://doi.org/10.1029/2002GC000433.

Lee, C.T.A., Luffi, P., Plank, T., Dalton, H., and Leeman, W.P., 2009, Constraints on the depths and temperatures of basaltic magma generation on Earth and other terrestrial planets using new thermobarometers for mafic magmas: Earth and Planetary Science Letters, v. 279, p. 20–33, https://doi.org/10.1016/j.epsl.2008.12.020.

Osozawa, S., Shinjo, R., Lo, C.H., Jahn, B.M., Hoang, N., Sasaki, M., Ishikawa, K., Kano, H., Hoshi, H., Xenophontos, C., and Wakabayashi, J., eds., 2012, Geochemistry and geochronology of the Troodos ophiolite: An SSZ ophiolite generated by subduction initiation and an extended episode of ridge subduction?: Lithosphere, v. 4, p. 497–510, https://doi.org/10.1130/L205.1.

Pearce, J.A., and Robinson, P.T., 2010, The Troodos ophiolitic complex probably formed in a subduction initiation, slab edge setting: Gondwana Research, v. 18, p. 60–81, https://doi.org/10.1016/j.gr.2009.12.003.

Portnyagin, M.V., Danyushevsky, L.V., and Kamenetsky, V.S., 1997, Coexistence of two distinct mantle sources during formation of ophiolites: A case study of primitive pillow lavas from the lowest part of the volcanic section of the Troodos Ophiolite, Cyprus: Contributions to Mineralogy and Petrology, v. 128, p. 287–301, https://doi.org/10.1007/s004100050309.

Portnyagin, M.V., Magakyan, R., and Schmincke, H.U., 1996, Geochemical variability of boninite magmas: Evidence from magmatic inclusions in highly magnesian olivine from lavas of southwestern Cyprus: Petrology, v. 4, p. 231–246.

Regelous, M., Haase, K.M., Freund, S., Keith, M., Weinzierl, C.G., Beier, C., Brandl, P.A., Endres, T., and Schmidt, H., 2014, Formation of the Troodos Ophiolite at a triple junction: Evidence from trace elements in volcanic glass: Chemical Geology, v. 386, p. 66–79, https://doi.org/10.1016/j.chemgeo.2014.08.006.

Sobolev, A.V., Dmitriev, L.V., Tsameryan, O.P., Kononkova, N.N., and Robinson, P.T., 1991, A possible primary melt composition for the ultramafic lavas of the Margi area, Troodos Ophiolite, in Gibson, I.L., Malpas, J., Robinson, P.T., and Xenophontos, C., eds., Cyprus Crustal Study Project Initial Report, Holes CY-1 and 1a, Paper 90-20, Geological Survey of Canada, p. 203–216.

Sun, S.S., and McDonough, W.F., 1989, Chemical and isotopic systematics of oceanic basalts: Implications for mantle composition and processes, in Saunders, A.D., and Norry, M.J., eds., Magmatism in the Ocean Basin: Geological Society, London, Special Publication 42, p. 313–345, https://doi.org/10.1144/GSL.SP.1989.042.01.19.

Woelki, D., Michael, P., Regelous, M., and Haase, K., 2020, Enrichment of H2O and fluid-soluble trace elements in the Troodos Ophiolite: Evidence for a near-trench origin: Lithos, v. 356, https://doi.org/10.1016/j.lithos.2019.105299.

Woelki, D., Regelous, M., Haase, K.M., and Beier, C., 2019, Geochemical mapping of a paleo-subduction zone beneath the Troodos Ophiolite: Chemical Geology, v. 523, p. 1–8, https://doi.org/10.1016/j.chemgeo.2019.05.041.

Woelki, D., Regelous, M., Haase, K.M., Romer, R.H.W., and Beier, C., 2018, Petrogenesis of boninitic lavas from the Troodos Ophiolite, and comparison with Izu–Bonin–Mariana fore-arc crust: Earth and Planetary Science Letters, https://doi.org/10.1016/j.epsl.2018.06.041.

APPENDIX

1. Calibration of the measure data of melt inclusion

1.1 Evidence of the Fe-loss process

The melt inclusion represents melt droplets which were trapped by mineral crystals growing in magma. However, composition of the melt inclusion still can be modified after the entrapment (Danyushevsky et al., 2000). In the case of olivine-host melt inclusions, post-entrapment-crystallization (PEC) process that the trapped melt crystallize olivine on the wall due to cooling is ubiquitous. If the cooling is very fast, PEC will produce a zoned rim and rapidly reduce the MgO contents and Mg# in the residual melt (Fig. A1). If the cooling is slow and therefore allows re-equilibration of the olivine rim on the walls and the olivine host, the zonation of the rim will be diminished until the olivine rim has the same compositions to the olivine host. As diffusion in the melt are faster than in the solid minerals, the residual melt would be also re-equilibrated. Such a re-equilibration process will cause rapid decrease in FeO content and increase in Mg# of the residual melt (Fig. A1). The re-equilibration process is therefore also named the Fe-loss process. Danyushevsky et al. (2000) illustrated that the Fe-loss process is ubiquitous in studies of melt inclusions. Similarly, this process is also identified in melt inclusions of this study. The evidence are as follows:

(1) The melt inclusions are clearly not equilibrated with their host olivines. Most equilibrated olivine of the melt inclusions, calculated by $K_D=[(X_{Fe}^{ol}X_{Mg}^{liq})/(X_{Mg}^{ol}X_{Fe}^{liq})]=0.3$, have lower Fo values than the host olivines of the melt inclusions

(Fig. A1). The difference can be explained by the combining effect of the PEC and iron-loss processes.

(2) When compared with the boninitic glasses and their inferred parental magma, the melt inclusions clearly have lower FeO_T contents, but other major elements largely overlap (Fig. A2). Moreover, it has been illustrated that, during the Fe-loss process, a negative correlation between the Fo of the host olivine and FeO_T content of the melt inclusion will be developed if inclusions from a magmatic suite are re-equilibrated equally. The negative trend is called as "Trend I" in the study of Danyushevsky et al. (2000), and is also identified in this study (Fig. A2).

1.2 Calibration through Petrolog3

Rehomogenization of the melt inclusions by the heating experiment could reverse the effect of PEC, but cannot resolve the effect of re-equilibration the re-equilibration (Fe-loss) process. To correct the effect of re-equilibration, a widely accepted method of Danyushevsky et al. (2000) was applied. The measured EPMA data of the melt inclusions were corrected to be in equilibrium with their host olivine through the Petrolog3 software (Danyushevsky and Plechov, 2011). Oxygen fugacity is set to be △QFM+0.8 according to the olivine-spinel oxybarometer of Ballhaus et al. (1991). The olivine model is after Ford et al. (1983).

To reconstruct the initially trapped melt composition, we need to specify the initial FeO_T content of the trapped melt. Most studies of melt inclusion tend to choose FeO_T values of primitive glass nearby or their inferred parental magma, it is because that

K_d(Fe) between high-Fo olivine and melt is usually very close to 1 and hence early crystallization of olivine limitedly affected the FeO_T content of the magma (Putirka, 2005). In this study, we follows this strategy and choose 8.4 wt.% as the original FeO_T content of the melt inclusion. This value comes from the inferred parental magma of the boninitic lavas in the Troodos ophiolite (Duncan and Green, 1980). Moreover, boninitic glass recovered in the Margi area have almost same FeO_T contents (8.2±0.1 wt.%) (Fig. A2).

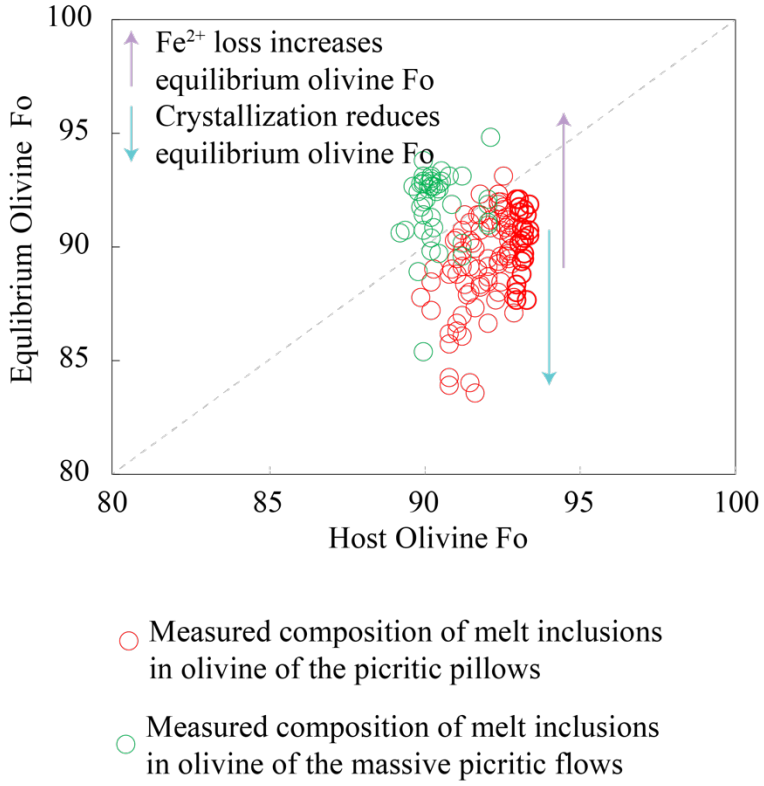

Figure A1. Comparison of the Fo of olivine in equilibrium with the melt inclusion against the Fo of the olivine host. Fo of the equilibrium olivine were calculated by measured data of melt inclusions with assuming $K_D=[(X_{Fe}^{ol}X_{Mg}^{liq})/(X_{Mg}^{ol}X_{Fe}^{liq})]=0.3$

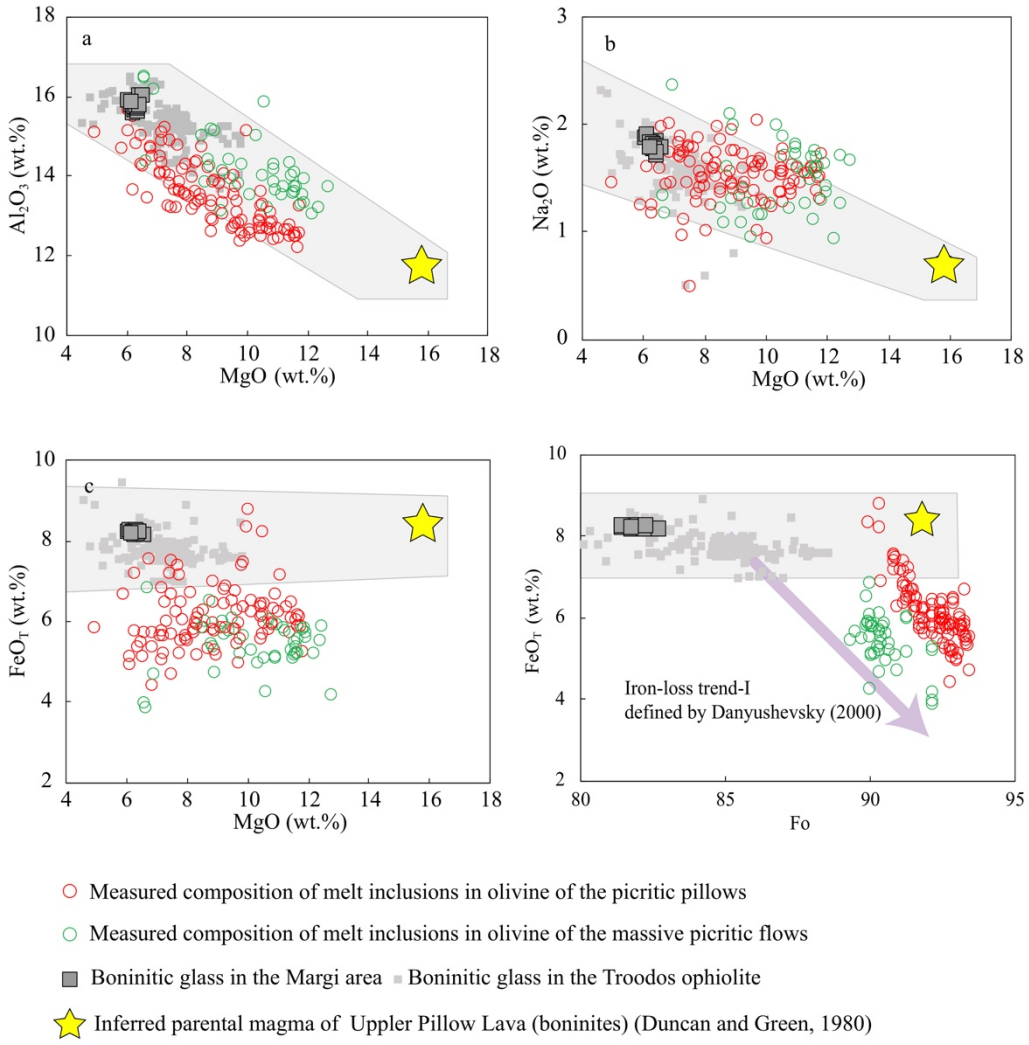

Figure A2. Comparison of the melt inclusion against the boninitic glass in the Troodos ophiolite. Data of the boninitic glass in the Troodos ophiolite are from Pearce and Robinson (2010), Osozawa et al. (2012), and Woelki et al. (2018, 2019 and 2020).

2. Boninites in the Troodos ophiolite

Lavas in the Troodos ophiolite are complex and highly variable. Multiple standards have been proposed to group the Troodos lava. The Geological Survey Department of Cyprus divided the pillow lava into the upper pillow lava (UPL) and the lower pillow lava (LPL) based on field observation across the ophiolite. In the landmark work on the Troodos lava, Miyashiro (1974) identified that the lavas of the Troodos ophiolite evolved in different trends, including an iron-enrich tholeiitic trend in LPL and a no-iron-enrich calc-alkalic trend in the UPL. Subsequent studies of fresh glasses confirm the existence of two major magma series in accordance with stratigraphic intervals (e.g., Robinson et al., 1983). The LPL is mainly composed of a series of tholeiitic magma with high TiO_2 contents, while the UPL comprises a series of boninitic magma with high MgO and low TiO_2 (Robinson et al., 1983, Pearce and Robinson, 2010). However, such chemostratigraphy is now being challenged by recent investigations on volcanic glasses, which suggest that (1) boninites are restricted in the southern part of the Troodos ophiolite (Woelki et al., 2019) and do not occur in the northern part and (2) boninites and tholeiitic basalts are interbedded, unlike the IBM forearc system (Woelki et al., 2018).

The melt inclusions in this study have typical boninite compositions. They are sampled from the Margi area, which is located in the northern flank of the Troodos ophiolite. Therefore, our study provides strong evidence of existence of boninites in the northern flank. Boninite is defined as volcanic rocks with high magnesium and silica contents

but low titanium contents (> 52 wt.% SiO_2, > 8 wt.% MgO and < 0.5 wt.% TiO_2) (Le Bas, 2000). It is highly possible that some evolved low-MgO volcanic glasses which were derived from boninitic magmas may be excluded from the boninite group if we simply and strictly define boninite as an individual rock type with special chemical composition sensu stricto. As suggested by Pearce and Robinson (2010) and Pearce and Reagan (2019), it is more reasonable to consider boninites as part of a series, i.e., boninite-HMA series. In the diagrams of SiO_2-MgO and MgO-TiO_2 (Fig. A3), some volcanic glass from the northern part (e.g., Kato Pyrgos, Peristerona, and Margi) are clearly within the range of the boninite-HMA series. Moreover, these glass have trace element compositions similar to melt inclusions in this study (Fig. A4), indicating that they were indeed evolved from boninitic magma.

The second point is based on volcanic glasses in the Parekklisia section where Woelki et al, (2018) proposed that tholeiitic basalts and boninites are interbedded. However, the Parekklisia "tholeiitic basalts" in their study have trace element compositions similar to that of boninitic melt inclusion in this study (Fig. A4). These "tholeiitic basalts" are also in the range of the boninite-HMA series (Fig. A3). These facts indicate that the Parekklisia "tholeiitic andesitic basalts" should be more evolved lavas of boninitic magma. On the other hand, the boninites in Woelki et al, (2018) belongs to the depleted boninite as defined in this study, with their low TiO_2 concentrations and fractionated trace element patterns (Figs. A3 and A4). Therefore, their study indeed suggests a interbed relationship between different types of boninites, rather than

between boninites and tholeiitic basalts. Their work complements existing knowledge of the relationship between the boninite and the depleted boninite which suggest that the depleted boninite erupted later than the boninite (Osozawa et al., 2012).

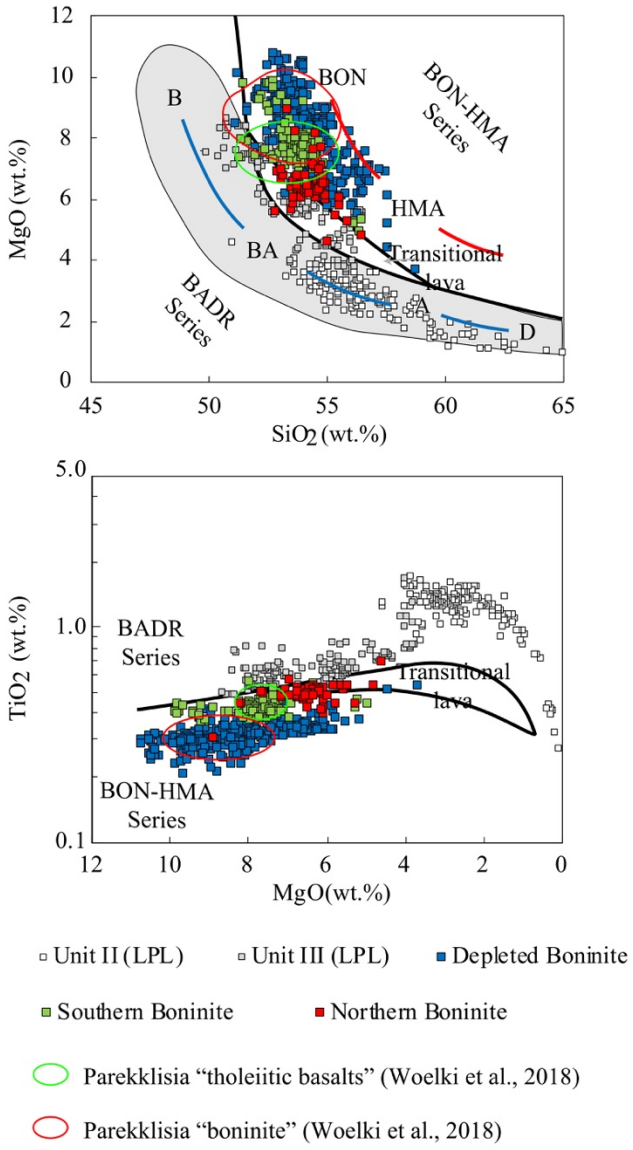

Figure A3. Major composition of volcanic glass in the Troodos ophiolite. Data are from Portnyagin et al. (1997), Pearce and Robinson (2010), Osozawa et al. (2012), Regelous et al. (2014), Woelki et al. (2018, 2019 and 2020), and Golowin et al. (2017).

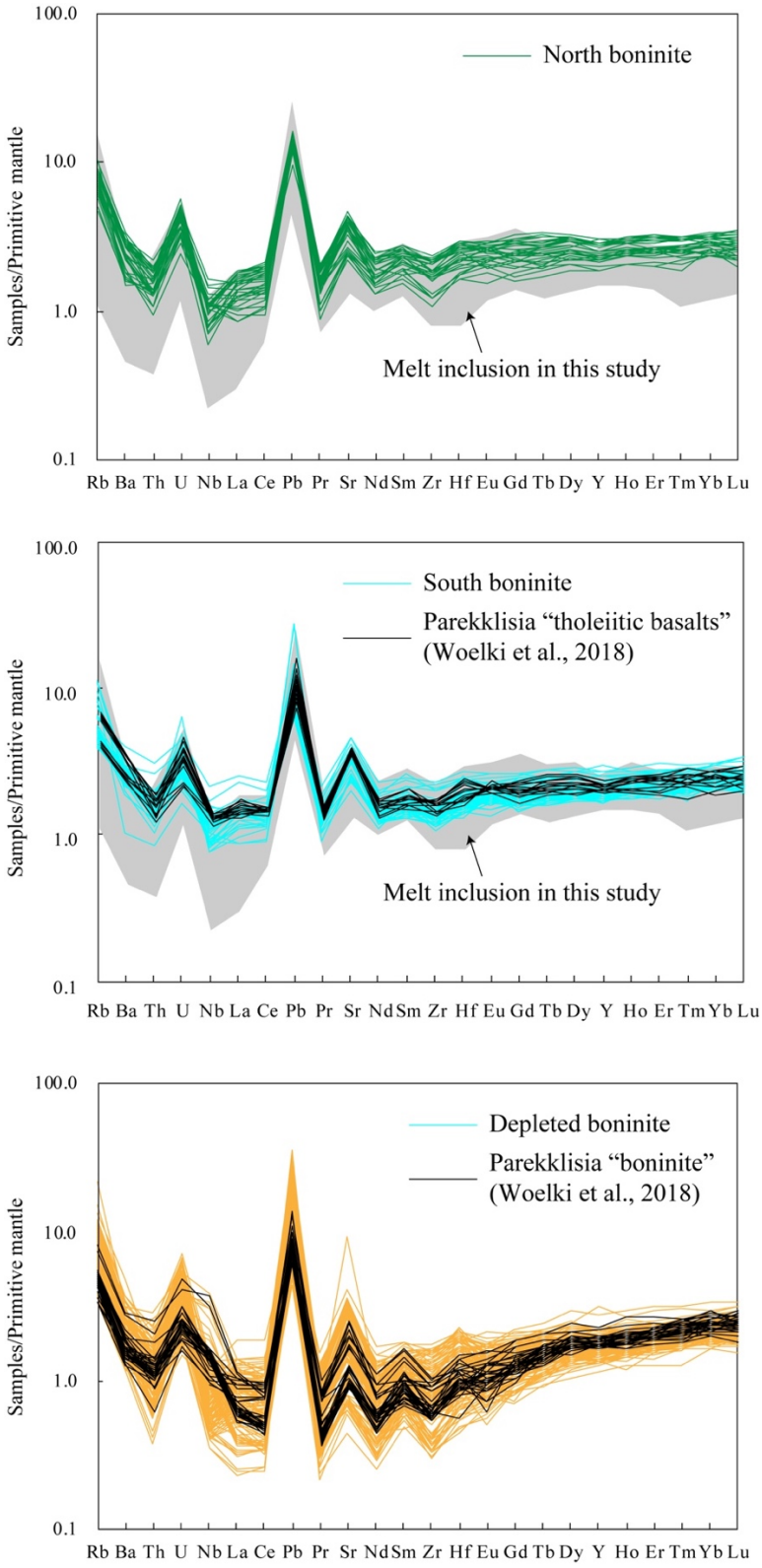

Figure A4. Primitive mantle normalized trace element patterns of the boninitic glass in the Troodos ophiolite. The normalization values are from Sun and McDonough (1989).

References

Ballhaus, C., Berry, R. F., and Green, D. H., 1991, High pressure experimental calibration of the olivine-orthopyroxene-spinel oxygen geobarometer: implications for the oxidation state of the upper mantle: Contributions to Mineralogy and Petrology, v. 107, p.27-40, doi: 10.1007/BF00311183

Danyushevsky, L. V., Della-Pasqua, F. N., and Sokolov, S., 2000, Re-equilibration of melt inclusions trapped by magnesian olivine phenocrysts from subduction-related magmas: petrological implications. Contributions to Mineralogy and Petrology, v. 138, p. 68-83, doi: 10.1007/PL00007664.

Danyushevsky, L.V., and Plechov, P., 2011, Petrolog3: Integrated software for modeling crystallization processes: Geochemistry Geophysics Geosystems, v. 12, Q07021, doi:10.1029/2011GC003516.

Duncan, R., and Green, D. H., 1980, Role of multistage melting in the formation of oceanic crust: Geology, v. 8, p. 22-26, doi: 10.1130/0091-7613(1980)8<22:ROMMIT>2.0.CO;2.

Ford, C. E., Russell, D. G., Craven, J. A., & Fisk, M. R., 1983, Olivine-liquid equilibria: temperature, pressure and composition dependence of the crystal/liquid cation partition coefficients for Mg, Fe2+, Ca and Mn: Journal of Petrology, v. 24, p. 256-266, doi: 10.1093/petrology/24.3.256.

Golowin, R., Portnyagin, M., Hoernle, K., Sobolev, A., Kuzmin, D., and Werner, R., 2017, The role and conditions of second-stage mantle melting in the generation of low-Ti tholeiites and boninites: the case of the Manihiki Plateau and the Troodos ophiolite: Contributions to Mineralogy and Petrology, v. 172, p. 104, doi: 10.1007/s00410-017-1424-3.

Le Bas, M. J., 2000, IUGS reclassification of the high-Mg and picritic volcanic rocks: Journal of Petrology, v. 41, p. 1467-1470, doi: 10.1093/petrology/41.10.1467.

140 Miyashiro, A., 1973, The Troodos ophiolitic complex was probably formed in an island
141 arc: Earth and Planetary Science Letters, v. 19, p. 218-224, doi: 10.1016/0012-
142 821X(73)90118-0.
143 Osozawa, S., Shinjo, R., Lo, C. H., Jahn, B. M., Hoang, N., Sasaki, M., ... and
144 Wakabayashi, J., 2012, Geochemistry and geochronology of the Troodos ophiolite:
145 An SSZ ophiolite generated by subduction initiation and an extended episode of
146 ridge subduction?: Lithosphere, v. 4, p. 497-510, doi: 10.1130/L205.1.
147 Putirka, K. D., 2005, Mantle potential temperatures at Hawaii, Iceland, and the mid-
148 ocean ridge system, as inferred from olivine phenocrysts: Evidence for thermally
149 driven mantle plumes: Geochemistry, Geophysics, Geosystems, v. 6, doi:
150 10.1029/2005GC000915.
151 Pearce, J. A., and Reagan, M. K., 2019, Identification, classification, and interpretation
152 of boninites from Anthropocene to Eoarchean using Si-Mg-Ti systematics:
153 Geosphere, v. 15, p. 1008-1037, doi: 10.1130/GES01661.1.
154 Pearce, J. A., and Robinson, P. T., 2010, The Troodos ophiolitic complex probably
155 formed in a subduction initiation, slab edge setting: Gondwana Research, v. 18, p.
156 60-81, doi: doi.org/10.1016/j.gr.2009.12.003.
157 Portnyagin, M. V., Danyushevsky, L. V., and Kamenetsky, V. S., 1997, Coexistence of
158 two distinct mantle sources during formation of ophiolites: a case study of
159 primitive pillow-lavas from the lowest part of the volcanic section of the Troodos
160 Ophiolite, Cyprus: Contributions to Mineralogy and Petrology, v. 128, p. 287-301,
161 doi: 10.1007/s004100050309.
162 Regelous, M., Haase, K.M., Freund, S., Keith, M., Weinzierl, C.G., Beier, C., Brandl,
163 P.A., Endres, T., and Schmidt, H., 2014, Formation of the Troodos Ophiolite at a
164 triple junction: Evidence from trace elements in volcanic glass: Chemical
165 Geology , v. 386, p. 66–79, doi: 10.1016/j.chemgeo.2014.08.006.

166 Robinson, P. T., Melson, W. G., O'Hearn, T., and Schmincke, H. U., 1983, Volcanic
167 glass compositions of the Troodos ophiolite, Cyprus: Geology, v. 11, p. 400-404,
168 doi: 10.1130/0091-7613(1983)11<400:VGCOTT>2.0.CO;2.
169 Woelki, D., Michael, P., Regelous, M., and Haase, K., 2020, Enrichment of H2O and
170 fluid-soluble trace elements in the Troodos Ophiolite: Evidence for a near-trench
171 origin: Lithos, v. 356, doi: 10.1016/j.lithos.2019.105299.
172 Woelki, D., Regelous, M., Haase, K. M., and Beier, C., 2019, Geochemical mapping
173 of a paleo-subduction zone beneath the Troodos Ophiolite: Chemical Geology, v.
174 523, p. 1-8, doi: 10.1016/j.chemgeo.2019.05.041.
175 Woelki, D., Regelous, M., Haase, K.M., Romer, R.H.W., and Beier, C., 2018,
176 Petrogenesis of boninitic lavas from the Troodos Ophiolite, and comparison with
177 Izu–Bonin–Mariana fore-arc crust: Earth and Planetary Science Letters,
178 doi:10.1016/j.epsl.2018.06.041.